

Ion transport in the fragile glass former $3\text{KNO}_3\text{-}2\text{Ca}(\text{NO}_3)_2$

A. Pimenov, P. Lunkenheimer, H. Rall, R. Kohlhaas, and A. Loidl
Institut für Festkörperphysik, Technische Hochschule, 64289 Darmstadt, Germany

R. Böhmer

Institut für Physikalische Chemie, Johannes Gutenberg-Universität, 55099 Mainz, Germany
and Institut für Festkörperphysik, Technische Hochschule, 64289 Darmstadt, Germany

(Received 17 November 1995)

The molten salt $3\text{KNO}_3\text{-}2\text{Ca}(\text{NO}_3)_2$ has been studied in the frequency range $5\text{ mHz} < \nu < 40\text{ GHz}$ and for temperatures $10\text{ K} < T < 500\text{ K}$ using impedance spectroscopy. It is found that in the microwave regime the dynamic conductivity traces the primary response. In the radio- and audio-frequency ranges the mobile ion relaxation becomes increasingly decoupled and the time scale and stretching of the response as determined from electrical modulus spectra differ from those obtained by spectroscopies probing the structural response. For $T > 360\text{ K}$ minima are detected in the dielectric loss that make possible a comparison with recent mode-coupling theories of the glass transition. The absence of analogous minima in nonionic supercooled liquids is discussed. [S1063-651X(96)09907-2]

PACS number(s): 64.70.Pf, 77.22.-d

I. INTRODUCTION

The study of simple prototypic supercooled liquids continues to be attractive since many phenomena associated with the glass transition are far from being completely understood. Metallic and ionic melts, as paradigms for hard-sphere systems, are particularly suitable for investigations on how the amorphous state is formed. This is mainly because of two reasons. On the one hand, recent mode-coupling theory [1–3] (MCT) aiming at enhancing our understanding of viscous liquids is generally thought to be applicable to these model systems. On the other hand, random close-packed melts belong to the class of fragile liquids [4]. Fragile liquids are those glass formers that show a large variability of medium-range order in their supercooled regime and hence pronounced temperature dependences in quantities such as the configurational entropy and the effective energy barriers against molecular or ionic rearrangements. Consequently, these materials exhibit particularly large thermodynamic anomalies in the glass transformation range as well as sizable deviations from simple thermally activated behavior [4].

The molten nitrates [5], among them the binary mixtures of potassium nitrate and calcium nitrate, are well studied ionic melts that approximate hard-sphere systems. They are relatively easy to vitrify since their eutectic phase diagram [6], reproduced as Fig. 1, shows that near the eutectic point a particularly high degree of undercooling relative to the pure compounds can be achieved. The composition $3\text{KNO}_3\text{-}2\text{Ca}(\text{NO}_3)_2$ (CKN) is the one that has been studied most extensively so far. The inset of Fig. 1 shows a schematic representation of the shape of the ions that constitute this substance. While K^+ and Ca^{2+} are spherical ions with the electronic configuration of argon, NO_3^- is a planar molecular ion of threefold symmetry with no permanent dipolar moment.

This structural simplicity makes CKN a material well suited for computer simulation studies [7,8]. It is also re-

markable that this model system was one of the first glass formers on which MCT was being tested, using the neutron spin-echo technique [9]. Subsequent neutron- [10] and light-scattering [11] studies on CKN have guided the refinements of this theory. Very recently we have shown that CKN is the first glass former [12] for which it was possible to test predictions of MCT using dielectric spectroscopy [13]. Numerous other experimental investigations have been conducted on CKN, focusing on various relaxation phenomena, e.g., using viscosimetric [14], mechanical [15,16], calorimetric [17–20], or optical methods [21–25].

The different experimental techniques can probe different degrees of freedom within the molten salt. Hence differences and similarities between the various experimental results can provide information about the extent to which different relaxational modes are coupled to one another. It has been argued that the existence of a large number of relaxation modes, active at a given temperature, is a characteristic feature of *fragile* glass formers [26]. It has been shown that the

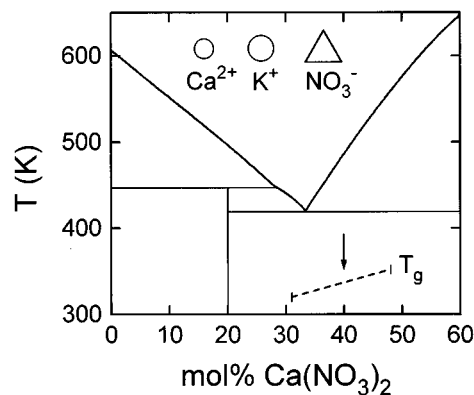


FIG. 1. Phase diagram of calcium and potassium nitrate (after Refs. [6] and [50]). The inset shows in a schematic fashion shapes and ionic radii of the K^+ , Ca^{2+} , and NO_3^- ions. The arrow marks the composition investigated in the present study.

dynamics of these modes, which are strongly coupled at temperatures far above the point of fusion, decouple sequentially from the primary structural response on approaching the calorimetric glass transition [27].

Among the modes decoupled from the primary one [19,28], particularly the rotational dynamics of the nitrate group has received much attention [29–31], above and slightly below room temperature. Deep in the glassy phase, the thermodynamic low-temperature anomalies have been examined [32,33]. The relation of these properties to the fragility of the melt has been explored [34].

The dynamics of that subset of ions which is mobile and which is responsible for the electrical conductivity has also been investigated. It is generally believed that the K^+ ions dominate the charge transport phenomenon [35], which is yet another example of motion decoupled from the primary response of CKN. Various aspects of the electrical relaxation properties of the mobile ions have been studied previously for different ranges of frequency [13,36–39]. It has become clear that electrode polarization effects often hamper the analysis of frequency-dependent data that have been discussed in terms of either the complex dielectric constant ϵ^* , the electrical modulus $M^*=1/\epsilon^*$, or the associated conductivity $\sigma=i\omega\epsilon_0\epsilon$. The frequency dependence of these quantities has been parametrized variously using the stretched exponential response function or likewise by power laws and Gaussian distributions of relevant quantities, for certain ranges of frequency. The situation encountered here is somewhat confusing due to the fact that there is an ongoing controversy as to which representation and description of electrical relaxation data is the most appropriate [40–46]. From conductivity data a frequency exponent s is usually extracted, while the width of the loss parts of modulus and dielectric susceptibility is often described in terms of a Kohlrausch or stretching exponent β .

For most *glassy* ionic conductors (i.e., below T_g) β is found to be insensitive to temperature, which is also the case for vitreous CKN [37]. Puzzling, however, is the temperature dependence of the width of the electrical modulus spectra of the supercooled *liquid*, which decreases upon cooling [37]. This is remarkable in two respects. On the one hand, the spectral widths measured for supercooled liquids almost always broaden as the temperature is lowered, although some exceptions are known [47,48]. On the other hand, a compilation of Kohlrausch exponents ($\beta \approx W^{-1}$, with W being the width of the imaginary part of M) measured on CKN shows that while the stretching exponent β_M determined from electrical relaxation experiments increases below a certain temperature, the exponents β from other experimental techniques remain small and decrease slightly with temperature [45]. Arguments to explain this startling behavior [49], which is thought to be connected with the phenomenon of decoupling [45], have been put forth. The question has been raised whether at high temperatures, for which the motions of the different kinds of ions are presumably coupled more strongly, the T dependence of β exhibits a more familiar behavior [48]. The temperature range for which a change in the T dependence of β_M may be expected has not been explored so far. The relevant conductivity relaxation process in this range can be estimated to lie in the microsecond to nanosecond regime. Therefore we have carried out radio-

frequency conductivity measurements. Additionally, we have taken data at audio-frequencies in order to be able to analyze the conductivity and relaxational behaviors of CKN in the glassy phase as well as in the supercooled liquid state.

This paper is organized as follows. After describing the experimental details in Sec. II we present the frequency- and temperature-dependent dielectric constants and conductivities in Sec. III. In Sec. IV we first treat the electrode polarization effects and then analyze our data in terms of the modulus formalism. We then present the temperature dependence of the stretching parameters as well as the relaxation map of CKN and discuss some implications. We conclude this section with a discussion of the high-frequency dielectric results of the nitrate glass and then, in Sec. V, summarize our findings.

II. EXPERIMENTAL DETAILS

The ingot chemicals KNO_3 (>99% purity), and $Ca(NO_3)_2 \cdot 4H_2O$ (>99% purity) from Merck Co. were fused and dehydrated at 510 K usually for at least one day in a vacuum furnace. The samples were then transferred immediately into a dry box and further handled under argon atmosphere. The glass transition temperature was checked using differential scanning calorimetry.

Most experiments in the liquid state were performed using a constant cooling rate of about 0.5 K/min. Since CKN exhibits an enhanced tendency to crystallize for temperatures in the vicinity of 390 K [50] here the measurements were carried out for cooling rates of about 2 K/min. The results were reproducible by heating runs for rates larger than about 2 K/min, but occasionally crystallization occurred even at those rates. The sub-audio-frequency measurements were carried out by equilibrating the melt at a temperature near 343 K and then cooling into the glassy phase with rates of about 10 K/min.

Standard capacitive probe heads were used in the sub-audio-, audio-, and radio-frequency ranges. The low-frequency measurements were taken with the frequency response analyzer Schlumberger 1260 in conjunction with the Chelsea dielectrics interface. The impedance analyzer Hewlett-Packard model HP4284 was used in the range $20 \text{ Hz} < \nu < 1 \text{ MHz}$. For frequencies $1 \text{ MHz} < \nu < 5 \text{ GHz}$ a reflection technique was used employing the HP4191 and the HP8510C network analyzers. At higher frequencies the data were taken in transmission geometry using the HP8510C equipped with various rectangular waveguides.

III. RESULTS

The temperature dependence of the logarithm of dielectric constant ϵ' and conductivity σ' of CKN is shown in Fig. 2 for $10 \text{ K} < T < 500 \text{ K}$ in a semilogarithmic representation. Both quantities show little temperature variations below the glass transition, but exhibit an increase by several orders of magnitude above T_g . In the liquid phase, the dielectric constant is strongly frequency dependent, as is typical for molten ionic conductors. The dramatic increase of ϵ' over some orders of magnitude for $T > 330 \text{ K}$ and low frequencies can be attributed to the formation of space charges near the electrodes ("blocking electrodes"). However, as is best seen for

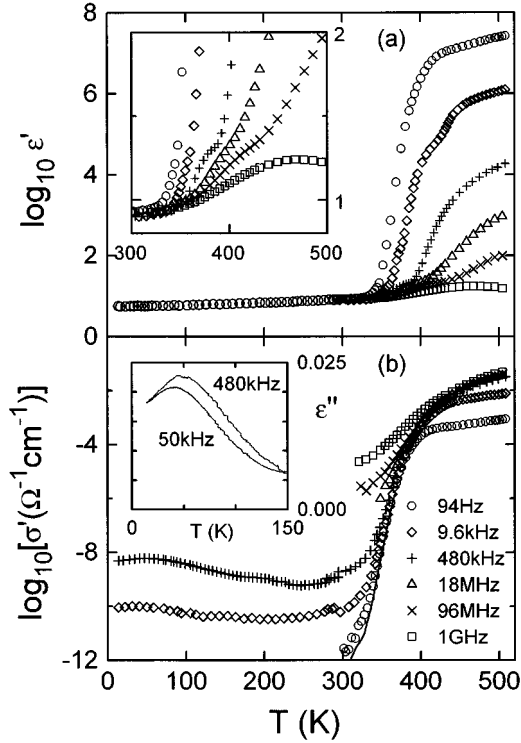


FIG. 2. Temperature dependence of the dielectric constant (upper frame) and electrical conductivity (lower frame) of CKN. The solid line in the lower frame represents the dc conductivity of the melt as taken from Ref. [37]. The upper inset gives an enlarged view of the logarithm of the dielectric constant for T above room temperature. Note that ϵ' , in particular at low frequencies, first increases moderately, due to a relaxation process, and then rises precipitously due to long-range ionic transport and the formation of space charges near the electrodes. The lower inset shows the low-temperature dielectric loss of the nitrate glass. The frequency-dependent loss peaks are indicative for a dipolar relaxation process.

intermediate frequencies, the dielectric constant tends to level off at moderate values of ϵ' before the huge increase over some orders of magnitude sets in, which can be attributed to a dielectric relaxation process. Only for the largest frequency shown, ϵ' is unaffected by the blocking electrode effects, which otherwise mask the dielectric relaxation at least partially.

The conductivity at low temperatures is strongly frequency dependent. Data for $T < 150$ K presented as dielectric loss $\epsilon'' = \sigma' / (\omega \epsilon_0)$ are displayed in the inset of the lower frame of Fig. 2. It is seen that for audio-frequencies maxima show up near $T = 50$ K that shift with ν . Similar indications for the existence of a low-temperature dielectric relaxation process have been obtained earlier [51]. Attempts to relate this phenomenon to a contamination of the sample with water impurities failed since we have not been able to affect it by different treatments of the melt such as incomplete dehydration. Since the ionic trace impurities present in our samples are likely to be different from those presumably present in the sample prepared by Hayler and Goldstein [51], it is suggested that the relaxation might be intrinsic.

Above T_g the measured conductivities approach the dc measurements taken from Ref. [37] and reproduced in the lower frame of Fig. 2 as solid line. At temperatures above

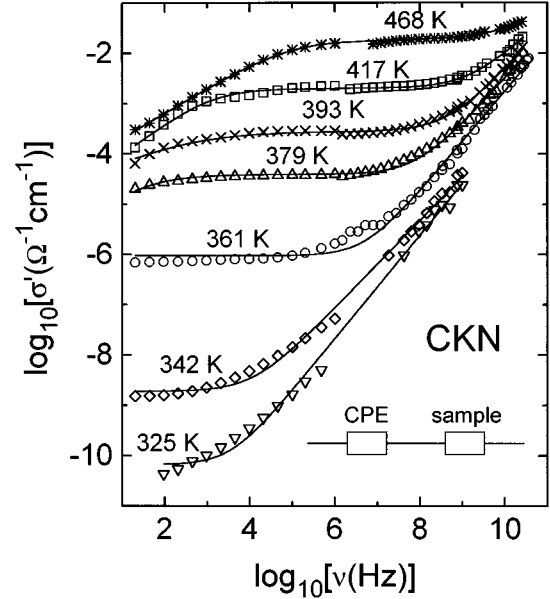


FIG. 3. Frequency-dependent electrical conductivity isotherms for several temperatures. The solid lines have been calculated using Eq. (2), which is based on the equivalent circuit shown as the inset. The sample characteristics are described using Eq. (3) and the electrode effects have been modeled using the constant phase admittance Y_C [Eq. (1)].

approximately 400 K the measured conductivities of CKN for low frequencies are smaller than $\sigma_{dc} \approx 0.01 \Omega^{-1} \text{ cm}^{-1}$. This phenomenon is due to the fact that the high conductivity facilitates the build-up of space charges near the blocking electrodes, an effect that also causes the huge increase of ϵ' at high temperatures as mentioned above.

Figure 3 shows the frequency dependence of σ' in a double-logarithmic representation. For the lower temperatures a frequency-independent dc plateau is followed by a power-law behavior $\sigma' \sim \omega^s$, with $s \leq 1$ a behavior that is often seen in ionic conductors. For temperatures $T \geq 379$ K the dc plateau is preceded by an increase of σ' with frequency that is also caused by the blocking of the electrodes by space-charge formation.

IV. ANALYSIS AND DISCUSSION

A. Conductivity spectra and electrode polarization

A closer inspection of the data presented in Fig. 2 reveals that the electrode polarization effects cannot be described by a purely capacitive element connected in series to the sample. A more general treatment of the blocking electrode problem [52] sometimes is possible with the constant phase element that is defined via its admittance [53]

$$Y_C = Y_0 (i\nu)^b, \quad (1)$$

where Y_0 is an adjustable parameter. The exponent b defines the *phase* of the element. The case of the pure capacitor is recovered for $b=1$; the Warburg impedance corresponds to $b=0.5$ [54]. If connected in series with the sample in a fashion depicted as the inset of Fig. 3, the measured complex conductance Y_m is

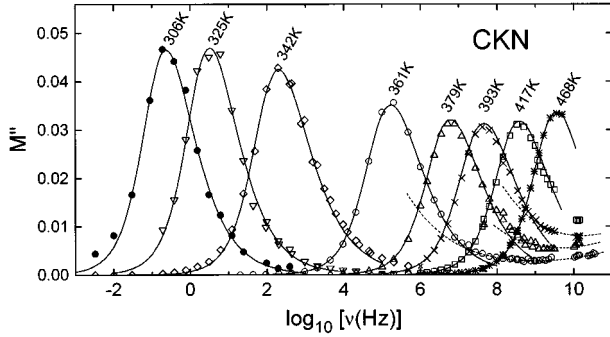


FIG. 4. Imaginary part of the electrical modulus $M''(\nu)$ of CKN. The solid lines are best fits using the stretched exponential, Eqs. (4) and (5). The dashed lines have been calculated using the mode-coupling equations discussed below.

$$Y_m = Y_C Y_s / (Y_C + Y_s). \quad (2)$$

Here Y_s denotes the (intrinsic) complex conductance of the molten salt. The frequency dependence of the complex conductivity $\sigma = Y_s d/A$ (with d the thickness and A the area of the sample) of ionic conductors is often described using the empirical expression [55]

$$\sigma(\nu) = \sigma_{dc} + A \nu^s + i A \nu^s \tan(s\pi/2), \quad (3)$$

where A and s are adjustable parameters. The results of least-square fits performed using this model are shown as solid lines in Fig. 3. The agreement of fits and measured curves is reasonably good, especially for the higher temperatures. However, as becomes obvious for the lower temperatures, the parametrization of the data is only moderately good in the transition region between the dc plateau and the power-law increase [56]. From the fits we find dc conductivities σ_{dc} consistent with those obtained in a previous study [37], the Warburg exponent $b = 0.5 \pm 0.05$, and a temperature-dependent slope parameter s . It increases from a value of about 0.7 at the highest accessible temperature ($T = 468$ K) to unity below about $T = 360$ K, thus resembling results obtained for a number of solid electrolytes [57]. However, caution is exercised when interpreting the apparent finding of an average low-temperature slope $s = 1$ in CKN (implying overall constant loss behavior) in terms of a so-called second universality [57]. This is because, when taking a closer look at the data at the highest frequencies investigated, a slope $s > 1$ shows up that is associated with a slight minimum of the dielectric loss. This minimum of $\epsilon''(\nu)$ is an important feature of our data, which will be discussed in detail in Sec. IV C.

B. Modulus spectra and decoupling phenomena

For the case of ionic conductors Macedo *et al.* have proposed the use of the modulus representation, which effectively leads to a suppression of the phenomena related to the dc conductivity and electrode polarization [52]. Figure 4 shows the imaginary part of the electrical modulus M'' obtained in this work for a broad range of frequencies. At low temperatures the modulus peaks are relatively narrow and broaden slightly upon heating. The double-peak structure reported in a previous study [38] cannot be confirmed by the

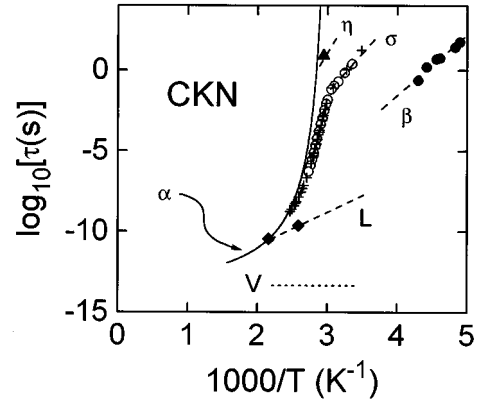


FIG. 5. Relaxation map of CKN. Primary relaxation times (solid line; see Ref. [25] for a compilation) are compared to results from conductivity relaxation (O, Ref. [37]; +, this work) and other decoupled processes: vibrational excitations (dotted line, Ref. [11]), rotational motion of the nitrate group (\blacklozenge , Ref. [29]), local chemical exchange (\blacktriangle , Ref. [19]), and Johari-Goldstein type of β relaxation detected by mechanical spectroscopy (\bullet , Ref. [28]). The dashed lines represent Arrhenius behaviors.

present data. From the peak maxima one usually defines a conductivity relaxation time via $\omega_p \tau_\sigma = 1$. It is seen that τ_σ is strongly temperature dependent and that near the glass transition at $T_g \approx 330$ K the peak frequency (and, equivalently, the conductivity relaxation rate) is *not* located at about 1 mHz, which would be expected if the conductivity relaxation would be fully coupled to the structural or α relaxation (cf. Fig. 8 in Ref. [37]).

In order to analyze the data one can use a formalism based on the stretched exponential function

$$\Phi(t) = \exp[-(t/\tau_\sigma)^{\beta_M}], \quad (4)$$

which yields [58]

$$M(\nu) = M_\infty \left[1 - \int \left(-\frac{d\Phi}{dt} \right) e^{-i2\pi\nu t} dt \right]. \quad (5)$$

Here $M_\infty = 1/\epsilon_\infty$ is the inverse of the high-frequency permittivity. From the relaxation time τ_σ and the Kohlrausch exponent β_M , the average conductivity relaxation time $\langle \tau_\sigma \rangle$ can be calculated using

$$\langle \tau_\sigma \rangle = \frac{\tau_\sigma}{\beta_M} \Gamma\left(\frac{1}{\beta_M}\right). \quad (6)$$

The Kohlrausch exponent has occasionally been related to the slope exponent s via $s = 1 - \beta$. As we have briefly discussed in Sec. IV A (see also Ref. [56]) and documented in detail elsewhere [59], such a relationship is not valid in general, but rather depends on the frequency range selected for analysis. Due to this reason the temperature dependence of the slope s will not be discussed further and in the following we shall focus attention on the fit parameters appearing in Eqs. (4) and (5), viz., the time-scale parameters and the coefficients describing amplitude and shape of the frequency response as given in Figs. 5 and 6, respectively. These figures also contain data taken from the literature.

Figure 5 shows the relaxation map of CKN. The conduc-

tivity relaxation time and the dc conductivity are proportional to one another in the entire temperature range. The data of this work slightly extend the range accessible to previous workers, but otherwise are fully compatible with literature values [37]. It is seen that the conductivity process traces the primary or α relaxation at high temperatures only. At intermediate temperatures the ion transport gradually decouples from the structural response. At T_g a clear break in slope of the τ_σ vs $1/T$ curve is seen. Below T_g the charge transport proceeds in an environment, which is essentially frozen on the time scale of the experiment, thus leading to a temperature-independent mean activation energy. Also other decoupled excitations (characterized below by the index i) such as the rotational motion of the nitrate group or the β relaxation obey Arrhenius laws $\tau_i = \tau_0 \exp(E_i/k_B T)$ with respective activation energies E_i . It is reassuring that the prefactors τ_0 of practically all processes turn out to lie in the vicinity of 10^{-15} s. Hence the data shown in Fig. 5 demonstrate that the effective energy barriers of the decoupled processes are larger the lower in temperature they decouple.

Grimsditch and Torell have argued that the existence of several relaxation processes present at a given temperature may be at the origin of the broad nonexponential response in fragile glass formers such as CKN [26]. This conjecture is indeed suggestive since relaxation maps as complex as the one shown in Fig. 5 are usually also observed in amorphous polymers, which exhibit pronounced deviations from simple Debye behavior. On the other hand, Fig. 5 also suggests that at high temperatures the spread in the distribution of relaxation times may decrease.

Figure 6 provides the rescaled amplitude parameter $1 - M_0/M_\infty$ [$M_0=0.056$ was estimated from the inverse static dielectric constant; cf. inset of Fig. 2(a)] as well as a compilation of stretching exponents β deduced from a variety of experiments. It is noted that the exponents presented in this figure were in some cases taken from measurements of susceptibilities, while in other cases from measurements of moduli.

The amplitude and stretching data from the present study compare reasonably well with those taken from Howell *et al.* in the temperature range where both sets of data overlap [37]. For $T < T_g$ our Kohlrausch exponents are somewhat smaller. Although we have to admit that the precision of the low-frequency data is not as good as that for the data taken at high frequencies, the absence of scatter in the Kohlrausch exponents suggests that the difference may be significant. This would be consistent with the fact that the cooling procedure employed in the present work led to a higher fictive temperature T_f of the glass than that obtained in Ref. [37] after an extended equilibration at $T_f=332.5$ K. For temperatures $T > 350$ K we find that the degree of stretching is constant with $\beta=0.62 \pm 0.03$. We suspect that the relatively steep decrease of the β values reported previously to continue for $T > 350$ K is due to the fact that in the earlier study [37] only frequencies below 1 MHz were accessible, i.e., the high frequency wing of the loss peak could not be measured in full detail.

The difference in the stretching parameters obtained from the conductivity study with respect to those reported from mechanical and other spectroscopies has extensively been discussed in the literature [45,60]. It may suffice to mention

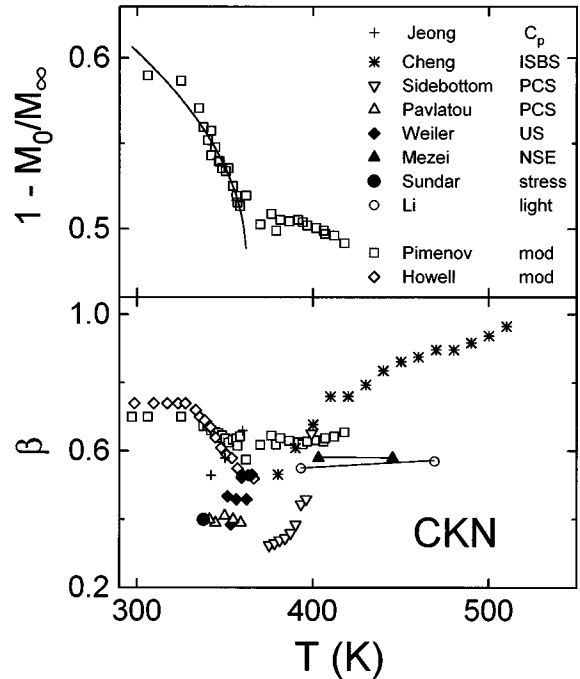


FIG. 6. Upper frame: amplitude factor M_∞ from our conductivity relaxation spectra rescaled by $M_0=0.056$. The solid line is inspired by MCT as described in Sec. IV C. Lower frame: shape parameter $\beta(T)$ as obtained from the analysis of the present data (\square) and compared with results from previous studies of conductivity relaxation (\diamond) [37], mechanical stress relaxation (\bullet) [16], enthalpy relaxation ($+$) [20], photon correlation spectroscopy (\triangle) [24,25], ultrasound (\blacklozenge) [15], neutron spin echo (\blacktriangle) [9], and impulsive stimulated Brillouin scattering ($*$) [23]. The Cole-Davidson parameters reported in the latter study were transformed to the corresponding Kohlrausch exponents according to Ref. [70].

here that this observation sometimes has been related to the phenomenon of conductivity decoupling. Therefore it is interesting to ask what happens when the decoupling ceases to exist, as is the case for temperatures above about 400 K (cf. Fig. 5). Figure 6 shows that at $T \approx 400$ K the Kohlrausch exponents from all studies agree. It is, however, also obvious that while the stimulated Brillouin scattering experiments [23] suggest that β approaches unity rapidly, the data from another light-scattering study [11] as well as from neutron scattering [9] and impedance spectroscopy are indicative of temperature-independent stretching. It is clear, however, that the conductivity relaxation has to be measured also at even higher frequencies and temperatures in order to see whether the ionic response returns to single exponential behavior in the highly fluid state.

C. Susceptibility minima and “microscopic peaks”

The minima in the loss part of the susceptibility are plotted in Fig. 7 together with corresponding results obtained by neutron- and light-scattering techniques [9,11]. In the overlapping frequency range all three sets of data are strikingly similar. This suggests that in molten salts the dielectric experiment strongly couples to density fluctuations, which in the case of CKN are thought to be probed by the other two techniques. Thus it appears possible that the present results can be used to test some predictions of mode coupling theory

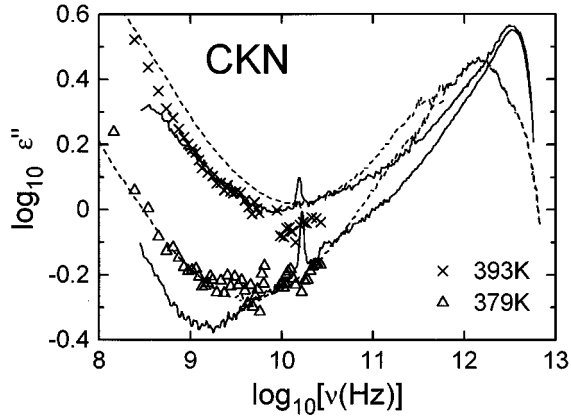


FIG. 7. High-frequency dielectric loss of CKN compared with results obtained using neutron scattering (dashed lines, Ref. [9]) and light scattering (solid lines, Ref. [11]) techniques. The neutron- and light-scattering data have been shifted along the ordinate axis to coincide with the dielectric data near 10 GHz.

[1,2]. Even the simplified version of MCT makes a number of specific statements concerning the minimum in the loss part of the dynamical susceptibility that approximately should be describable using the sum of two power laws

$$\varepsilon''(\nu) = \frac{\varepsilon''_{\min}}{a+b} \left[a \left(\frac{\nu}{\nu_{\min}} \right)^{-b} + b \left(\frac{\nu}{\nu_{\min}} \right)^a \right]. \quad (7)$$

According to the theory, the various parameters appearing in this formula are given by

$$\varepsilon''_{\min} \propto (T - T_C)^{0.5}, \quad (8)$$

$$\nu_{\min} \propto (T - T_C)^{1/2a}. \quad (9)$$

Furthermore, the exponents a and b are constrained by the so-called exponent parameter λ via

$$\lambda = \frac{\Gamma^2(1-a)}{\Gamma(1-2a)} = \frac{\Gamma^2(1+b)}{\Gamma(1+2b)}. \quad (10)$$

Hence the coefficient λ and the critical temperature T_C are to be treated as adjustable parameters in the framework of the theory. Once these coefficients have been determined experimentally, the time scale of the α process is predicted to be

$$\nu_{\max} \propto (T - T_C)^\gamma \quad \text{with} \quad \gamma = \frac{1}{2a} + \frac{1}{2b}. \quad (11)$$

The dielectric loss curves exhibiting a minimum could consistently be fitted using the exponents $a=0.23$ and $b=0.35$ yielding an exponent parameter $\lambda=0.87$ (Fig. 8) [13]. Using the same values, the dashed lines in Fig. 4 were calculated and are seen to describe also the modulus spectra quite well in the minimum regime. The temperature dependence of the scaling coefficients ν_{\min} and ε''_{\min} is shown in Fig. 9. It is seen that the behavior of both quantities is compatible with the predictions of MCT as implied by Eqs. (8) and (9) if T_C is

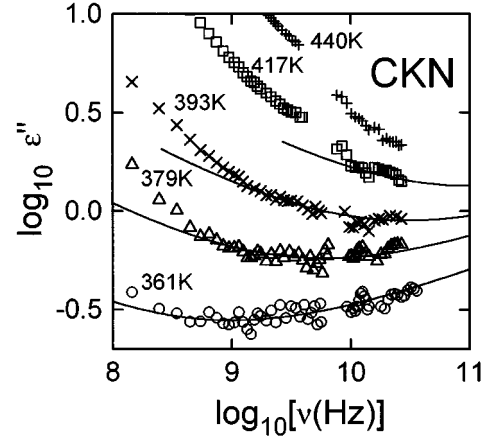


FIG. 8. Dielectric loss of CKN as measured at high frequencies. The solid lines represent fits using Eq. (7) with $a=0.23$ and $b=0.35$. Deviations between fits and data at low frequencies are due to dc and ac conductivity.

chosen to be about 360 K. This temperature is close to that obtained by previous studies [9,11].

A nontrivial consequence of the minimum scaling is that theoretically the susceptibility maximum should follow Eq. (11) with $\gamma=0.28=\frac{1}{3.6}$. Since for CKN it is evident that ν_{\max} is masked by the strong dc conductivity, we have plotted in Fig. 9(c) the maxima taken from the modulus spectra. This procedure may be justified by noting that in glass-forming liquids for which maxima in the loss parts of both modulus and susceptibility can be resolved and in particular for temperature-independent stretching as is the case here, the ratio of the peak frequencies is usually well defined [41,61].

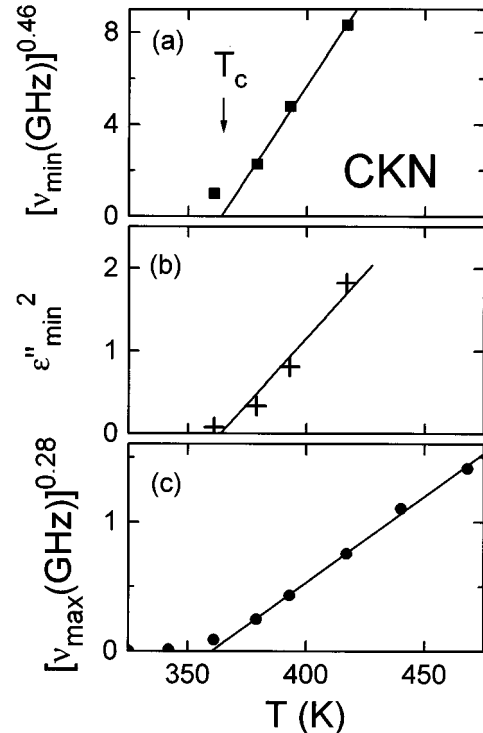


FIG. 9. Temperature dependence of various parameters obtained from the analysis of the high-frequency data in terms of MCT. The solid lines are consistent with a critical temperature of 360 K.

Figure 9 demonstrates clearly that $\nu_{\max}^{0.28}$ obtained this way varies linearly with temperature in a broad range. Another prediction of MCT that can be confirmed by resorting to the modulus spectra obtained in this work is that the stretching of the response is temperature independent for $T > T_C$. A statement of MCT that concerns the temperature range below T_C is that the Debye-Waller factor f_q should follow a square-root dependence $f_q = f_c + h_q[(T_C - T)/T_C]^{0.5}$. In the zero-wave-vector limit relevant for impedance spectroscopy one has $f_{q \rightarrow 0} = 1 - M_0/M_\infty$ [1]. The effective Debye-Waller factor (sometimes called the nonergodicity parameter) as determined using this formula, is shown in the upper frame of Fig. 6. A square-root fit describes our $f_{q \rightarrow 0}$ data reasonably well (solid line) and yields $T_C = 362 \pm 3$ K, consistent with our previous analysis, and a plateau value $f_c = 0.48 \pm 0.02$, in accord with the experimentally determined ratio of $(M_\infty - M_0)/M_\infty$ for $T > T_C$. Thus our somewhat limited set of data is consistent with the predictions of MCT.

The interpretation that emerges on the basis of the present findings is that the feedback mechanism invoked by the theory and often visualized by the so-called cage effect may be at work in CKN: The rattling motion of a cation, say, against the cage of its neighboring anions is, on the one hand, obviously connected with fluctuations of the local density. On the other hand, it is related with fluctuations of local dipole moments that are directly monitored using dielectric spectroscopy. Therefore it is argued that in fused salts density fluctuations are effectively probed by this type of experiment.

While the interpretation of the susceptibility minima in terms of mode-coupling theory is quite appealing, other potential explanations shall briefly be discussed in the following. The first consideration starts from the fact that for many if not all glass formers a broad far-infrared (FIR) absorption band is observable, which sometimes is termed microscopic peak. The tails of these absorption peaks should of course be observable, even in the gigahertz range, when the losses due to the α process have shifted out of this spectral range. The remaining losses may, however, be very small, rendering their detection difficult. It has recently been pointed out that the mechanical absorption in the FIR ($\alpha_{\max} \approx 5 \times 10^{-7}$ Np/cm at 10 THz) is by several orders of magnitude larger than the corresponding electrical absorption and that, more importantly, the strength of the microscopic peak relative to that of the α process is much stronger in the mechanical case [45,62]. This assignment of relative strengths to the low frequency and the microscopic absorptions is also supported by some preliminary FIR absorption data taken on CKN [63]. On the other hand, the relatively low constant loss absorption sketched in Ref. [63] suggests that minima in the dielectric loss may be located at an exceptionally low (gigahertz) frequency. Thus the high-frequency wing of the susceptibility minimum could be associated with the low-frequency tail of the microscopic peak, which often depends approximately quadratically on frequency, although other functional forms have been discussed [64,65].

Such steep frequency dependences should, however, be borne out by the data shown in Figs. 7 and 8 if the transition matrix element, which couples the FIR absorptions to the vibrational excitations, is frequency independent [64]. For several amorphous systems Strom and Taylor have provided

evidence that this matrix element might be correlated with the excess T^3 contributions to the specific heat [66], which in turn are related to the fragility of the glass formers [34]. It has to be noted, however, that these considerations are probably not sufficient to rationalize the finding of susceptibility minima, in general, as exemplified by fragile glass formers such as, e.g., polystyrene [64] and propylene carbonate [67] for which the FIR responses are known. More detailed investigations are warranted since this latter substance, which behaves anomalously in several other respects [68], exhibits a relatively small FIR absorption, although being about as fragile as CKN. On the other hand, sodium trisilicate, as an example of another prototypical ionic system, exhibits a very strong FIR absorption [64] suggesting that the ionicity of the bonding in the glass-forming material may be relevant.

As yet another potential explanation for the occurrence of susceptibility minima in CKN we would like to mention that, recently, Ngai has pointed out to us that, in the microwave range, the stretching of the response and therefore the cooperativity implied by the coupling scheme is much higher in CKN as compared to nonionic liquids. According to his scheme, the variations in the strength of the microscopic peak and the time scale of the cooperativity crossover are expected to lead to an enhancement of the absorption level relative to those seen in less coupled complex systems [69]. Hence the nonexponentiality (at microwave frequencies) rather than the fragility is thought to be associated with minima in the susceptibility.

V. SUMMARY AND OUTLOOK

In this work we have measured the dielectric response of supercooled CKN over a broad range of temperature and frequency. At low temperature (and below 1 MHz) our results are consistent with those obtained by previous authors [37,39] and confirm that the conductivity relaxation is decoupled from the primary one. In the megahertz range and above the Kohlrausch exponent obtained from the modulus spectra is practically temperature independent.

Another major finding of the present work is the observation of minima in the loss parts of the electrical modulus and susceptibility. We have shown that the shape as well as the temperature dependence of this phenomenon are in reasonable agreement with corresponding results from light- and neutron-scattering experiments. We have also shown that our high-frequency data are consistent with statements implied by recent versions of the mode-coupling theory. For a more detailed check of the theory by impedance spectroscopy it is necessary either to extend the measurements to even higher frequencies or to increase the sensitivity of the experiments in the gigahertz range. Efforts in both directions are currently under way [13].

Another possible option is to vary the size of the cations. Substitution of K by Rb, say, should couple the response of the mobile ions more tightly to that of the structure as a whole and consequently should lead to a slowing down of the conductivity response at a given viscosity. Thus it is expected that, in this case, several interesting phenomena effectively can be shifted towards lower frequencies into a more accessible frequency range. Experiments along these lines are planned to be reported elsewhere [33].

ACKNOWLEDGMENTS

This project was partly supported by the Deutsche Forschungsgemeinschaft (SFB 262). We thank Austen Angell, W. Götze, and Kia Ngai for very stimulating

discussions and Connie Moynihan for making parts of Ref. [39] available to us. The assistance of A. Maiazza with sample preparation is also gratefully acknowledged. Ingo Alig is thanked for the opportunity to carry out DSC experiments in his laboratory.

- [1] W. Götze and L. Sjögren, *Rep. Prog. Phys.* **55**, 241 (1992).
- [2] G. Mazenko, *J. Non-Cryst. Solids* **172–174**, 1 (1994).
- [3] W. Kob and H. C. Anderson, *Phys. Rev. E* **52**, 4134 (1995).
- [4] C. A. Angell, in *Relaxations in Complex Systems*, edited by K. L. Ngai and G. B. Wright (Naval Research Laboratory, Washington, DC, 1984), p. 3.
- [5] E. Thilo, C. Wieker, and W. Wieker, *Silikattechnik* **15**, 109 (1964).
- [6] A. Dietzel and H. P. Poegel, in *Proceedings of the International Glass Congress, Venice, 1953*, edited by A. Garzanti (Nella Stabilimento Grafico di Roma Delle, Rome, 1953), p. 219.
- [7] C. A. Angell and L. M. Torell, *J. Chem. Phys.* **78**, 937 (1983).
- [8] G. F. Signorini, J.-L. Barrat, and M. L. Klein, *J. Chem. Phys.* **92**, 1294 (1990).
- [9] F. Mezei, W. Knaak, and B. Farago, *Phys. Rev. Lett.* **58**, 571 (1987); in *Dynamics of Disordered Materials*, edited by D. Richter, A. J. Dianoux, W. Petry, and J. Teixeira (Springer, Berlin, 1989), p. 64.
- [10] W. Petry and J. Wuttke, *Transp. Theor. Stat. Phys.* **24**, 1075 (1995).
- [11] G. Li, W. M. Du, X. K. Chen, H. Z. Cummins, and N. Z. Tao, *Phys. Rev. A* **45**, 3867 (1992); H. Z. Cummins, G. Li, W. M. Du, J. Hernandez, and N. Z. Tao, *J. Phys. Condens. Matter* **6**, 52 (1994).
- [12] The so-called β minimum so far could not be detected in dielectric measurements below 40 GHz on polymers and insulating supercooled liquids; see, e.g., A. Hofmann, F. Kremer, E. W. Fischer, and A. Schönhals, in *Disorder Effects on Relaxational Processes*, edited by R. Richert and A. Blumen (Springer, Berlin, 1994), p. 309; P. K. Dixon, N. Menon, and S. R. Nagel, *Phys. Rev. E* **50**, 1717 (1994); P. Lunkenheimer, A. Pimenov, B. Schiener, R. Böhmer, and A. Loidl, *Europhys. Lett.* **33**, 611 (1996).
- [13] P. Lunkenheimer, A. Pimenov, R. Kohlhaas, R. Böhmer, and A. Loidl (unpublished).
- [14] H. Tweer, N. Laberge, and P. B. Macedo, *J. Am. Ceram. Soc.* **54**, 121 (1971).
- [15] R. Weiler, R. Bose, and P. B. Macedo, *J. Chem. Phys.* **53**, 1258 (1970).
- [16] H. G. K. Sundar and C. A. Angell, in *Collected Papers of the XIVth International Congress on Glass, New Delhi, 1985* (Indian Ceramic Society, Calcutta, 1986), Vol. II, pp. 161–168; C. A. Angell, *J. Non-Cryst. Solids* **102**, 205 (1988).
- [17] C. T. Moynihan, H. Sasabe, and J. C. Tucker, in *Proceedings of the International Symposium on Molten Salts*, edited by J. P. Pennsler, J. Bronstein, D. R. Morris, K. Nobe, and W. P. Richards (Electrochemical Society, Pennington, NJ, 1976), p. 182.
- [18] B. Büchner and P. Korpiun, *Appl. Phys.* **43**, 29 (1987).
- [19] R. Böhmer, E. Sanchez, and C. A. Angell, *J. Phys. Chem.* **96**, 9089 (1992).
- [20] Y. H. Jeong and I. K. Moon, *Phys. Rev. B* **52**, 6381 (1995).
- [21] J. Wong and C. A. Angell, *J. Non-Cryst. Solids*, **7**, 109 (1972).
- [22] M. Grimsditch, R. Bhadra, and L. M. Torell, *Phys. Rev. Lett.* **62**, 2616 (1989).
- [23] L.-T. Cheng, Y.-X. Yan, and K. A. Nelson, *J. Chem. Phys.* **91**, 6052 (1989).
- [24] D. L. Sidebottom and C. M. Sorensen, *J. Chem. Phys.* **91**, 7153 (1989).
- [25] E. A. Pavlatou, A. K. Rizos, G. N. Papatheodorou, and G. Fytas, *J. Chem. Phys.* **94**, 224 (1991).
- [26] M. Grimsditch and L. M. Torell, in *Dynamics of Disordered Materials*, edited by D. Richter, A. J. Dianoux, W. Petry, and J. Teixeira (Springer, Berlin, 1989), p. 196.
- [27] C. A. Angell, *J. Non-Cryst. Solids* **131–133**, 15 (1991).
- [28] C. Mai, S. Etienne, J. Perez, and G. P. Johari, *Philos. Mag. B* **50**, 657 (1985).
- [29] P. Jacobsson, L. Börjesson, A. K. Hassan, and L. M. Torell, *J. Non-Cryst. Solids* **172–174**, 161 (1994).
- [30] M. Ricci, P. Foggi, R. Righini, and R. Torre, *J. Chem. Phys.* **98**, 4892 (1993).
- [31] T. Kamiyama, K. Shibata, K. Suzuki, and Y. Nakamura, *J. Non-Cryst. Solids* **192–193**, 272 (1995).
- [32] A. K. Raychaudhuri and R. O. Pohl, *Phys. Rev. B* **25**, 1310 (1982).
- [33] A. Pimenov, P. Lunkenheimer, M. Nicklas, R. Böhmer, and A. Loidl (unpublished).
- [34] A. P. Sokolov, A. Kisliuk, D. Quitmann, A. Kudlik, and E. Rössler, *J. Non-Cryst. Solids* **172–174**, 138 (1994).
- [35] A. Barkatt and C. A. Angell, *J. Phys. Chem.* **71**, 2192 (1975).
- [36] E. Rhodes, W. E. Smith, and A. R. Ubbelohde, *Trans. Faraday Soc.* **63**, 1943 (1967).
- [37] F. S. Howell, R. A. Bose, P. B. Macedo, and C. T. Moynihan, *J. Phys. Chem.* **78**, 631 (1974).
- [38] K. Funke, J. Hermeling, and J. Kümpers, *Z. Naturforsch. Teil A* **43**, 1094 (1988).
- [39] F. S. Howell, Ph. D. thesis, The Catholic University, Washington, DC, 1972 (unpublished).
- [40] A. Doi, *Solid State Ionics* **31**, 227 (1988).
- [41] G. P. Johari and K. Pathmanathan, *Phys. Chem. Glasses* **29**, 219 (1988).
- [42] C. T. Moynihan, *J. Non-Cryst. Solids* **172–174**, 1395 (1994).
- [43] R. H. Cole and E. Tombari, *J. Non-Cryst. Solids* **131–133**, 969 (1991).
- [44] S. R. Elliott, *J. Non-Cryst. Solids* **170**, 97 (1994).
- [45] C. A. Angell, *Chem. Rev.* **90**, 523 (1990).
- [46] I. Svare, F. Borsa, D. R. Torgeson, S. W. Martin, and H. Patel, *J. Non-Cryst. Solids* **185**, 297 (1995).
- [47] I. M. Hodge and C. A. Angell, *J. Chem. Phys.* **67**, 4 (1977).
- [48] W. C. Hasz, C. T. Moynihan, and P. A. Tick, *J. Non-Cryst. Solids* **172–174**, 1363 (1994).

- [49] K. L. Ngai, R. W. Rendell, A. K. Rajagopal, and S. Teitler, *Ann. N. Y. Acad. Sci.* **484**, 150 (1984).
- [50] H. Senapati, R. K. Kadiyala, and C. A. Angell, *J. Phys. Chem.* **95**, 7050 (1991).
- [51] L. Hayler and M. Goldstein, *J. Chem. Phys.* **66**, 4736 (1977).
- [52] P. B. Macedo, C. T. Moynihan, and R. Bose, *Phys. Chem. Glasses* **13**, 171 (1972).
- [53] *Impedance Spectroscopy—Emphasizing Solid Materials and Systems*, edited by J. R. MacDonald (Wiley, New York, 1987).
- [54] E. Warburg, *Ann. Phys. Chem.* **67**, 493 (1899).
- [55] A. K. Jonscher, *Dielectric Relaxation in Solids* (Chelsea Dielectrics, London, 1983).
- [56] Restricting the analysis to a limited frequency range can naturally lead to better fits using Eq. (3); however, the question of the reliability of the fitting parameters has to be raised. See D. L. Sidebottom, P. F. Green, and R. K. Brow, *J. Non-Cryst. Solids* **183**, 151 (1995).
- [57] W. K. Lee, J. F. Liu, and A. S. Nowick, *Phys. Rev. Lett.* **67**, 1559 (1991).
- [58] C. T. Moynihan, L. P. Boesch, and N. L. Laberge, *Phys. Chem. Glasses* **14**, 122 (1973).
- [59] R. Böhmer, P. Lunkenheimer, M. Lotze, and A. Loidl, *Z. Phys. B* (to be published).
- [60] K. L. Ngai and J. N. Mundy, in *The Physics of Non-Crystalline Solids*, edited by L. D. Pye, W. C. LaCourse, and H. J. Stevens (Taylor and Francis, London, 1992), p. 342.
- [61] M. A. Floriano and C. A. Angell, *J. Chem. Phys.* **91**, 2537 (1989).
- [62] C. A. Angell and R. Böhmer, in *Applications of Mechanical Spectroscopy in Materials Science*, edited by L. B. Magalas (Elsevier, Amsterdam, in press).
- [63] C. A. Angell, in *Molten Salt Chemistry*, Vol. 202 of *NATO Advanced Study Institute, Series B: Physics*, edited by G. Mamtov and R. Marassi (Plenum, New York, 1987), p. 123.
- [64] U. Strom, J. R. Hendrickson, R. J. Wagner, and P. C. Taylor, *Solid State Commun.* **15**, 1871 (1977).
- [65] L. I. Deich, *Phys. Rev. B* **49**, 109 (1994).
- [66] U. Strom and P. C. Taylor, *Phys. Rev. B* **16**, 5512 (1977), Fig. 8.
- [67] C. A. Angell, L. Boehm, M. Oguni, and D. L. Smith, *J. Mol. Liq.* **56**, 275 (1993).
- [68] R. Böhmer, K. L. Ngai, C. A. Angell, and D. J. Plazek, *J. Chem. Phys.* **99**, 4201 (1993).
- [69] K. L. Ngai (private communication).
- [70] C. P. Lindsey and G. D. Patterson, *J. Chem. Phys.* **73**, 3348 (1980).